

1 **A machine learning approach to predict mortality and pulmonary hypertension severity in**
2 **newborns with congenital diaphragmatic hernia**

3

4 *Mortality and pulmonary hypertension prediction in congenital diaphragmatic hernia*

5

6 Luana Conte^{1,2†}, Ilaria Amodeo^{3†}, Giorgio De Nunzio^{2,4*}, Genny Raffaelli³, Irene Borzani⁵, Nicola
7 Persico^{6,7}, Alice Griggio⁸, Giuseppe Como³, Mariarosa Colnaghi³, Monica Fumagalli^{3,6}, Donato
8 Cascio^{1†}, Giacomo Cavallaro^{3†}

9

10 ¹Department of Physics and Chemistry, Università degli Studi di Palermo, Palermo, Italy

11 ²Advanced Data Analysis in Medicine (ADAM), Laboratory of Interdisciplinary Research Applied to
12 Medicine (DReAM), Local Health Authority (ASL) Lecce and Università del Salento, Lecce, Italy

13 ³Neonatal Intensive Care Unit, Fondazione IRCCS Ca' Granda Ospedale Maggiore Policlinico, Milan, Italy

14 ⁴Department of Mathematics and Physics "E. De Giorgi", Laboratory of Biomedical Physics and Environment,
15 Università del Salento, Lecce, Italy

16 ⁵Pediatric Radiology Unit, Fondazione IRCCS Ca' Granda Ospedale Maggiore Policlinico, Milan, Italy

17 ⁶Department of Clinical Sciences and Community Health, Università degli Studi di Milano, Milan, Italy

18 ⁷Department of Obstetrics and Gynecology, Fondazione IRCCS Ca' Granda, Ospedale Maggiore Policlinico,
19 Milan, Italy

20 ⁸Department of Obstetrics and Gynecology, ASST Fatebenefratelli Sacco, Ospedale Macedonio Melloni,
21 Milan, Italy

22

23 ***Corresponding Author.** Giorgio De Nunzio, giorgio.denunzio@unisalento.it

24 † Co-First Author: Luana Conte and Ilaria Amodeo

25 † Co-Last Author: Donato Cascio and Giacomo Cavallaro

26

27

28 Luana Conte: luana.conte@unipa.it, ORCID: <https://orcid.org/0000-0002-8741-3478>

29 Ilaria Amodeo: ilaria.amodeo@policlinico.mi.it, ORCID: <https://orcid.org/0000-0002-2650-0084>

30 Giorgio De Nunzio*: giorgio.denunzio@unisalento.it, ORCID: <https://orcid.org/0000-0002-1998-0286>

31 Genny Raffaelli: genny.raffaelli@policlinico.mi.it, ORCID: <https://orcid.org/0000-0001-9175-9394>

32 Irene Borzani: irene.borzani@policlinico.mi.it, ORCID: <https://orcid.org/0000-0003-0386-4712>

33 Nicola Persico: nicola.persico@unimi.it, ORCID: <https://orcid.org/0000-0001-9028-9597>

34 Alice Griggio: alicegriggio89@gmail.com, ORCID <https://orcid.org/0000-0002-2947-4627>

35 Giuseppe Como: pinocomo@gmail.com, ORCID: <https://orcid.org/0009-0009-2120-0427>

36 Mariarosa Colnaghi: mariarosa.colnaghi@policlinico.mi.it, ORCID:

37 Monica Fumagalli: monica.fumagalli@policlinico.mi.it, ORCID: <https://orcid.org/0000-0002-0186-0710>

38 Donato Cascio: donato.cascio@unipa.it, ORCID: <https://orcid.org/0000-0001-6522-1259>

39 Giacomo Cavallaro: giacomo.cavallaro@policlinico.mi.it, ORCID: <https://orcid.org/0000-0002-4921-1437>

40

41

42

43

44

45 **ABSTRACT**

46 Prenatal prediction of postnatal outcomes in newborns with congenital diaphragmatic hernia (CDH)
47 remains challenging, especially for mortality and neonatal persistent pulmonary hypertension
48 (PPHN). Despite the increasing utilization of advanced artificial intelligence (AI) technologies in the
49 neonatal field, this study is pioneering in exploring AI methodologies in the context of CDH. It
50 represents an initial attempt to implement a Machine Learning (ML) system to predict postnatal
51 mortality and PPHN severity, using prenatal and early postnatal data as input variables. We enrolled
52 50 patients with isolated left-sided CDH from singleton pregnancies and retrospectively collected
53 clinical and imaging variables from fetal ultrasound (US) and shape features extracted from magnetic
54 resonance imaging (MRI), combined with gestational age and birth weight. A supervised ML model
55 for predicting mortality and PPHN severity was developed, achieving good accuracy (88% for
56 mortality prediction and 82% for PPHN) and sensitivity (95% for mortality and 85% for PPHN). The
57 area under the curve (AUC) of the ROC curve was 0.88 for mortality and 0.82 for PPHN predictions.
58 Our results may lead to novel AI applications in the neonatal field, focusing on predicting postnatal
59 outcomes based on prenatal data, ultimately improving prognostic assessments and intervention
60 strategies for such a complex disease.

61 **Clinical Trial Registration:** The trial was registered at ClinicalTrials.gov with Identifier
62 NCT04609163

63

64 **Keywords:** Newborn, Congenital Diaphragmatic hernia, Neonatal Persistent Pulmonary
65 Hypertension, Mortality, Machine Learning, Deep Learning.

66

67

68 **What is Known:** prenatal prediction of postnatal mortality and severity of pulmonary hypertension
69 in CDH newborns remains challenging and largely based on imaging through the volumetric
70 assessment of fetal lungs.

71

72 **What is New:** developing a ML system for predicting PPHN severity and mortality risk based on the
73 integrated assessment of prenatal and early postnatal variables is feasible, with good accuracy.

74

75 INTRODUCTION

76 Congenital diaphragmatic hernia (CDH) is a rare congenital anomaly characterized by incomplete
77 closure of the diaphragm and herniation of abdominal organs into the chest, resulting in pulmonary
78 hypoplasia, neonatal persistent pulmonary hypertension, and cardiac dysfunction [1–3]. CDH occurs
79 in nearly 1 in 2500 births. Several factors influence the prognosis, such as defect size and location,
80 associated anomalies, presence of liver up in the thorax, and gestational age at birth [4,5]. Risk
81 stratification is essential to identify patients who might benefit from specific interventions and to
82 enable a risk-adjusted analysis of outcomes, healthcare costs, and management approaches. Prenatal
83 and postnatal CDH predicting tools have largely increased and have been validated during the last
84 years based on clinical and instrumental data [6,7,16–18,8–15]. However, a universal risk
85 stratification method has not been identified yet, and an agreed-upon set of risk-specific management
86 guidelines is still lacking [19].

87 In particular, predicting the severity of Neonatal Persistent Pulmonary Hypertension (PPHN) using
88 conventional prenatal diagnostic methods remains challenging. As a result, there is growing interest
89 in leveraging advanced technologies that favor a timely and accurate prognosis.

90 Artificial Intelligence (AI) is increasingly applied in the neonatal field to support medical data
91 analysis. Predictive algorithms are being developed using traditional Machine Learning (ML)
92 approaches as well as its more advanced Deep Learning (DL) extension. ML and DL can process and
93 analyze medical data, including images from different sources such as ultrasound, magnetic
94 resonance imaging (MRI), and X-ray. Integrating these algorithms into healthcare systems holds
95 promise for enhancing diagnostic accuracy and disease pattern classification. These algorithms could
96 help predict specific outcomes, guide interventions, and improve the overall quality of care
97 [20,21,30,22–29].

98 However, to our knowledge, these methodologies still need to be successfully applied to newborns
99 with CDH. The aim of our study was to provide a predictive algorithm for mortality and PPHN in
100 CDH based on the integrated analysis of prenatal and early postnatal data.

101 **MATERIALS AND METHODS**

102 *Study design*

103 This study represents an exploratory secondary analysis of a retrospective cohort study performed at
104 Fondazione IRCCS Ca' Granda Ospedale Maggiore Policlinico, Milan, Italy (CLANNISH, Clinical
105 Trials identification n°: NCT04609163) [29]. The study involved the following services: the Fetal
106 Surgery Center, Pediatric Radiology Service, and Neonatal Intensive Care Unit (NICU). Moreover,
107 the Department of Mathematics and Physics at the Università del Salento (Lecce, Italy) and the
108 Department of Physics and Chemistry at the Università degli Studi di Palermo (Palermo, Italy)
109 developed the AI algorithms.

110 The current study adhered to the principles of good clinical practice and followed the guidelines of
111 the Helsinki Declaration. It received approval from the local ethics committee (Milan Area 2, Italy)
112 with approval number/ID 800_2020bis. However, considering its retrospective design, the ethics
113 committee waived the need for informed consent. The study was also registered on ClinicalTrials.gov
114 with the identifier NCT04609163.

115

116 *Patients*

117 The study population, inclusion-exclusion criteria, and a comprehensive description of the primary
118 study design were previously published and are briefly summarized here [29]. Inborn CDH patients
119 born between 01/01/2016 and 30/04/2020 admitted to the NICU at birth were included. The take-
120 charge of the mothers took place at our Fetal Surgery Center at a gestational age of 30+6 weeks or
121 below. Non-isolated CDH and twin pregnancies were excluded. Only left-sided CDH were
122 considered because of their larger numerosity, homogeneity, and variability in liver position, leaving
123 out right-sided CDH.

124 A total of 50 patients were included in the final study population.

125

126 *Data Collection*

127 Clinical maternal and fetal prenatal variables were retrospectively collected using Astraia software
128 (Astraia Software GmbH, Ismaning, Germany) and NeoCare software (GPI SpA, Trento, Italy). A
129 prenatal ultrasound (US) performed between 25+0 and 30+6 weeks of gestation was considered for
130 each patient. In the case of fetal endoscopic tracheal occlusion (FETO), the fetal US was performed
131 before the fetal procedure. Additionally, native sequences from fetal MRI were gathered for 36 out
132 of 50 cases, with separate acquisitions for the lung and liver. The imaging software employed for this
133 study was Synapse PACS and Synapse 3D (FUJIFILM Medical Systems, Lexington, MA, US). Lung
134 volumes were computed using T2 HASTE sequences, selecting the best-quality image plane without
135 motion-induced artifacts [31]. On the other hand, liver volumes were calculated based on T1 VIBE
136 sequences [32]. An experienced pediatric radiologist (IB) freehand delineated Regions Of Interest
137 (ROIs) to define the areas of the left and right lungs and the liver, excluding the pulmonary hila and
138 mediastinal structures for each slice. Organ volumes were calculated using the software.
139 Subsequently, the DICOM (Digital Imaging and Communications in Medicine) files were
140 anonymized and converted to the NIfTI (neuroimaging informatics technology initiative) format for
141 easy manipulation.

142 *Clinical and Imaging variables*

143 A detailed summary of the clinical and imaging variables included is reported in Table 1.

144

Table 1. Clinical and imaging variables
<i>Maternal data</i> Mother age Ethnicity Number of gestations ending the outcome for fetuses with an Assisted Reproduction (MAR): yes/no Antenatal use of corticosteroids: yes/no Premature rupture of membranes (pPROM): yes/no Gestational age at pPROM Gestational age at CDH diagnosis
<i>Fetal ultrasound data</i> Gestational age Estimated Fetal Weight the (EFW) Amniotic Fluid (AF) Umbilical Artery Pulsatility Index

Pulmonary Flow Pulsatility Index Pulmonary flow Peak Systolic Velocity Peak early diastolic reversed flow Organ herniation of Bowel, Stomach, Liver: yes/no Observed/expected lung-to-head ratio (tracing method) CDH severity: mild, moderate, severe Fetal Endoscopic Tracheal Occlusion (FETO): yes/no Gestational age at balloon insertion and removal
<i>MRI data</i> Gestational age Apparent diffusion coefficient (ADC) Right and left lung volume Total fetal lung volume (TFLV) Observed/expected TFLV (O/E TFLV%) Total liver volume Herniated Liver volume Percentage of liver herniation (%LH) Mediastinal shift angle (MSA) Apparent diffusion coefficient (ADC) of the left and right lung
<i>Early postnatal data</i> Gestational age at birth Birth weight

145

146 *Radiomics features*

147 In addition to the clinical variables, standard 3D radiomics features were extracted from the
 148 segmented ROIs in the MRI using the freely available and open-source Pyradiomics v. 3.01 software
 149 tool [30,33]. Pyradiomics produces many variables, with and without preprocessing by various filters
 150 and optional reslicing, with different interpolators. Only features from the original images without
 151 preprocessing were considered in this work. Due to significant dissimilarity in the gray-level content
 152 of the MRI scans, only shape features were utilized (MeshVolume, VoxelVolume, SurfaceArea,
 153 SurfaceVolumeRatio, Sphericity, Maximum3DDiameter, MajorAxisLength, MinorAxisLength,
 154 LeastAxisLength, Elongation, and Flatness). The geometric meaning of each feature is detailed in
 155 Table 2.

156

Table 2. Geometric meaning of Pyradiomics shape features	
Feature	Geometric Meaning

MeshVolume	The shape volume, calculated using a mesh representation. It is the three-dimensional space enclosed by the surface of the object.
VoxelVolume	The volume calculated by counting the number of voxels (3D pixels) within the shape and multiplying by the volume of a single voxel. This represents the discretized volume of the object.
SurfaceArea	The total area of the surface of the shape. This quantifies the two-dimensional extent of the object's surface.
SurfaceVolumeRatio	The ratio of surface area to volume. This measure indicates how 'compact' an object is; lower values suggest a more compact shape.
Sphericity	A measure of how spherical (round) the object is. Perfect spheres have a sphericity of 1. Lower values indicate less spherical shapes.
Maximum3DDiameter	The largest distance between any two points on the surface of the shape. This is the maximum length of the object in any dimension.
MajorAxisLength	The length of the major axis of the shape, which is the longest dimension in the principal component analysis (PCA) of the object.
MinorAxisLength	The length of the minor axis, which is perpendicular to the major axis and is the second longest dimension in the PCA of the object.
LeastAxisLength	The shortest axis length from the PCA of the object. It's perpendicular to both the major and minor axes.
Elongation	The ratio of the minor axis length to the major axis length. It indicates how much longer the shape is in one direction compared to the other.
Flatness	The ratio of the least axis length to the major axis length. This measure indicates how 'flat' or 'elongated' an object is compared to being spherical.

157

158 Variables computed from the gray levels were discarded, avoiding additional image manipulation,
 159 such as intensity standardization. A total of 80 features were considered: 56 prenatal variables, 2 very
 160 early postnatal variables as gestational age and birth weight, and 22 MRI-extracted shape features (11
 161 from the lungs, 11 from the liver).

162 To ensure fairness in the classification process, the features were normalized to the 0-1 range using
 163 min-max normalization on the training set. The same normalization parameters were then applied to
 164 the validation set samples. However, in some cases, the lack of MRI data resulted in missing values
 165 in the features extracted by Pyradiomics. This was also observed for non-radiomics features based on

166 the patient's diagnostic pathway. Imputation by a weighted average was considered [34] to handle
167 these missing values, as in Equation 1:

$$f_n(m) = \frac{\frac{\overline{f_n^{(1)}}}{\sigma_n^{(1)}} + \frac{\overline{f_n^{(2)}}}{\sigma_n^{(2)}}}{\frac{1}{\sigma_n^{(1)}} + \frac{1}{\sigma_n^{(2)}}} \quad (1)$$

168

169 where $f_n(m)$ is the value to be assigned to the (missing) n -th feature for the m -th sample, $\overline{f_n^{(1)}}$ and
170 $\overline{f_n^{(2)}}$ are the average values of the n -th features for classes 1 and 2, respectively, and $\sigma_n^{(1)}$ and $\sigma_n^{(2)}$ are
171 the corresponding standard deviations. This way, in the approximation of Gaussian distributions, a
172 neutral value for the distributions of the two classes is used as the missing feature.

173

174 *Target variables: neonatal persistent pulmonary hypertension and mortality*

175 For each included patient, a neonatologist performed a systematic revision of the first available
176 echocardiogram within 24 hours after birth, focusing on direct and indirect signs of pulmonary
177 hypertension. Data collection was focused on the presence and characteristics of the shunts through
178 patent ductus arteriosus and *foramen ovale*, the characteristics of the intraventricular sept, the
179 estimation of the systolic pulmonary artery pressure through tricuspid valve regurgitation, the
180 systemic pressures, and concomitant use of pulmonary vasodilators. Patients were then stratified
181 according to the presence and severity of pulmonary hypertension into two categories: severe (over-
182 systemic, considered as the positive class) vs moderate/mild (iso/under-systemic). According to
183 mortality, the study population was divided into non-survivors (positive class) vs survivors.

184

185 *Feature selection*

186 We employed the Recursive Feature Elimination (RFE) technique with Cross-Validation (CV),
187 specifically using the Leave One Patient Out CV (LOPO-CV) scheme. The RFE method starts with

188 the entire feature set and recursively removes the minor essential features based on a chosen metric
189 (in this case, accuracy) until the desired number of features is reached. Typically, the final number
190 of features to select is a parameter that needs to be specified. This parameter was determined
191 dynamically by varying its value and calculating the corresponding accuracy in our approach. We
192 then selected the parameter value that maximized accuracy. The Random Forest (RF) classifier was
193 used to evaluate the various configurations.

194

195 *Training*

196 To exploit the available samples as much as possible, we used a LOPO-CV scheme. In this method,
197 we selected one patient as the validation set while using the remaining patients for training. We
198 trained several classifiers and obtained performance metrics such as the confusion matrix, sensitivity,
199 specificity, area under the ROC curve (AUC), and the area under the P-R curve. All the optimization
200 steps were based on maximizing accuracy.

201

202 *Classifiers*

203 Three classification algorithms were tested: eXtreme Gradient Boosting (XGBoost), Support Vector
204 Machine (SVM), and K-Nearest Neighbors (KNN). The first classifier was used because it natively
205 and effectively deals with missing clinical values. The choice of the other two classifiers was due to
206 their ability to allow good performance in conditions of a limited number of available samples, as
207 they are characterized by a reduced number of parameters to be tuned [35]. Hyperparameter tuning
208 was performed to avoid overfitting and improve model performance.

209

210 **RESULTS**

211 The final study population consisted of 50 patients: 26 severe (52%) and 24 moderate/mild (48%)
212 cases of PPHN. According to mortality, 37 survivors (74%) and 13 non-survivors (26%) were present.

213 As regards mortality analysis, the feature selection procedure led to the choice of 10 out of 80 features,
214 in particular: maternal age, gestational age at CDH diagnosis, CDH severity (mild, moderate, severe),
215 centile of estimated fetal weight (EFW), observed/expected lung to head ratio (o/e LHR) by tracing
216 method, umbilical artery pulsatility index, left and right fetal lung volume (FLV) at MRI,
217 observed/expected total fetal lung volume (o/e TFLV), gestational age at birth, and birth weight.
218 Remarkably, no shape features were selected. Table 3 shows the classification results obtained for
219 mortality prediction.

220

Table 3. Classification figures of merit for mortality, computed in a LOPO scheme				
<i>Classifier</i>	<i>AUC</i>	<i>Accuracy</i>	<i>Sensitivity</i>	<i>Specificity</i>
XGBoost	0.88	88%	95%	69%
SVM	0.78	80%	97%	31%
KNN	0.78	82%	95%	46%

LOPO: Leave One Patient Out; KNN: K-Nearest Neighbors; SVM: Support Vector Machine; XGBoost: eXtreme Gradient Boosting.

221

222 The results of the different classification methods were comparable regarding AUC and accuracy,
223 though XGboost had better performance. Figure 1 shows the ROC and P-R curves for mortality
224 prediction obtained by XGboost with feature selection. The trained model correctly identified 88%
225 of cases and achieved a sensitivity of 95% and a specificity of 69%. The AUC from the ROC curve
226 was 0.87, while the P-R curve subtended an area of 0.95 (with the frequency of positive cases equal
227 to 52%). From the P-R curve, precision drops after 50% sensitivity but remains more than 85% when
228 sensitivity is 90%, and even if we require complete sensitivity, precision remains relatively high
229 (around 80%).

230

231 **Fig 1.** Mortality prediction. Left: ROC curve, right: P-R curve, obtained with the XGBoost classifier
232 on prenatal clinical variables. No shape features extracted from MRIs were used, as required by the
233 feature selection procedure.

234

235 As far as PH is concerned, feature selection led to the identification of the 14 features, in particular:
236 gestational age at CDH diagnosis, liver position, grading of stomach herniation, gestational age at US
237 ultrasound, centile of EFW, umbilical artery pulsatility index, peak early diastolic reversed flow, o/e
238 TFLV, apparent diffusion coefficient of left lung, original shape elongation, gestational age at birth,
239 and birth weight.

240 In this case, both clinical and shape features were selected. Table 4 reports the classification results
241 obtained for PPHN classification. The results produced by the different classification methods show
242 that XGboost also performed better in this case.

243 The XGboost classifier demonstrated significantly superior classification capabilities to the other two
244 classifiers (Tables 3 and 4).

Table 4. Classification figures of merit for PPHN, computed in a LOPO scheme				
Classifier	AUC	Accuracy	Sensitivity	Specificity
XGBoost	0.82	82%	85%	79
SVM	0.75	74	79	71
KNN	0.65	54	53	33

LOPO: Leave One Patient Out; KNN: K-Nearest Neighbors; PPHN: Neonatal Persistent Pulmonary Hypertension; SVM: Support Vector Machine; XGBoost: eXtreme Gradient Boosting.

245

246 Figure 2 shows the ROC and P-R curves for PPHN classification obtained by XGboost with the
247 features selection. The AUC from the test ROC curve was 0.82, while the P-R curve subtended an
248 area of 0.75 (with the frequency of positive cases equal to 26%). The trained model correctly
249 identified 82% of cases and achieved a sensitivity of 85% and a specificity of 79%. From the P-R

250 curve, we deduce that even at very high sensitivity values (about 83-84%), precision is more than
251 80%.

252

253 **Fig 2.** Left: the ROC curve; right: the Precision-Recall (P-R) curve for PPHN predictions with the
254 XGBoost classifier on prenatal clinical variables and shape features extracted from MRIs.

255

256 **DISCUSSION**

257 Congenital diaphragmatic hernia (CDH) is a life-threatening anomaly requiring high-skilled and
258 multidisciplinary team of experts for appropriate management since from antenatal diagnosis [36].

259 Despite advancements over time, morbidity and mortality remain significant (20–40%), even within
260 high-volume tertiary referral centers [37–39]. An estimated quarter of survivors experience
261 neurodevelopmental impairments across all domains, encompassing motor and sensory (hearing,
262 visual) deficits as well as cognitive, language, and behavioral impairments [40].

263 CDH patients exhibit varying degrees of pulmonary hypoplasia and abnormal pulmonary vascular
264 disease, resulting in varying extents of pulmonary hypertension. Up to 30–40% of newborns with
265 CDH experience concomitant cardiac ventricular dysfunction [41,42]. PPHN is associated with
266 adverse outcomes in CDH patients, underscoring the critical nature of its management in the care of
267 these infants [43].

268 Various clinical and laboratory parameters and prognostic indices in the perinatal period have been
269 subject to study to predict postnatal outcomes [39,44–47]. The identification of variables predictive
270 of mortality is paramount for clinical decision-making and parental guidance. The o/e LHR and o/e
271 TFLV serve as pivotal metrics in this regard. Each of these parameters evaluates the extent of
272 pulmonary hypoplasia associated with CDH, a critical determinant of both survival and long-term
273 prognosis.

274 The o/e LHR has been widely studied and utilized in the prediction of postnatal survival in cases of
275 isolated CDH. Jani et al. highlighted the significance of the o/e LHR in predicting survival in fetuses

276 with isolated diaphragmatic hernia [48]. Snoek et al. further assessed the predictive value of the o/e
277 LHR for survival and chronic lung disease (CLD) in survivors with left-sided CDH, reflecting its
278 ongoing relevance in an era of standardized neonatal treatment [49]. Their multicenter study
279 underscores the evolving understanding of o/e LHR in predicting outcomes for CDH patients.

280 On the other hand, the o/e TFLV exhibits a stronger correlation with postnatal outcomes than the
281 absolute lung volume. Moreover, a growing body of evidence supports the superior accuracy of o/e
282 TFLV in predicting survival compared to ultrasound-based estimations of lung size, which may not
283 fully account for the ipsilateral lung and could thus underestimate the effective lung volume [50–55].
284 In cases of isolated CDH, o/e TFLV has demonstrated efficacy in distinguishing survival, with an o/e
285 TFLV < 25% being associated with more severe forms and a reduced survival rate [54,56–60].
286 Furthermore, o/e TFLV has been shown to forecast the necessity for extracorporeal membrane
287 oxygenation (ECMO) after birth, with the combined assessment of lung volumetry and o/e LHR
288 proving more effective than ultrasound alone in predicting the need for ECMO [61–64].

289 Prenatal prediction of PPHN plays a crucial role in prenatal management, delivery planning and
290 postnatal care. However, while both o/e LHR and o/e TFLV offer insights into the extent of CDH-
291 associated pulmonary hypoplasia, their predictive value for PPHN necessitates careful consideration.
292 Our findings support the possibility of successfully developing a ML system for predicting PPHN
293 severity and mortality risk based on the integrated assessment of prenatal and early postnatal
294 variables.

295 To achieve our goal, we enrolled 50 left-sided CDH cases. The dataset was relatively balanced
296 concerning PPHN, with 26 severe and 24 moderate/mild cases, whereas mortality classes included
297 37 survivors and 13 non-survivors. We combined prenatal clinical and imaging data with gestational
298 age and weight at birth, which both play a key role in survival in neonatal patients, especially those
299 in critical conditions. In addition, standard 3D radiomics features were extracted from the segmented
300 ROIs using the freely available Pyradiomics software tool. This software package facilitated
301 automatic reslicing with a selected interpolator and computed multiple radiomics variables. As the

302 MRIs exhibited significant variations in grayscales, which would have required some form of
303 intensity standardization to use features based on gray values, we only utilized shape features to avoid
304 additional image manipulation and discarded variables based on the gray levels.

305 A feature selection phase was executed for both postnatal target variables, mortality, and PPHN. The
306 RFE approach used RF classification to evaluate different configurations, which was appropriate for
307 several reasons. First, this approach provides features of relative importance during the training
308 process. Each time a decision tree is constructed, the model tracks how much each feature contributes
309 to reducing the cost function, usually Gini impurity or entropy. An importance score for each feature
310 is obtained by averaging this importance across all trees. Second, because of its "forest" nature, a RF
311 is robust and less prone to overfitting than individual decision trees. This means that the computed
312 importance of features is more reliable and less affected by noise in the data. Finally, RFs can handle
313 highly correlated features without special preprocessing. In the presence of correlations, this approach
314 can distribute importance among correlated features, providing a complete picture of each feature
315 contribution.

316 We conducted a comprehensive evaluation of three classification algorithms: XGBoost, SVM, and
317 KNN. Our models were trained using prenatal and early postnatal clinical variables, as well as
318 selected shape features extracted from MRI data. Interestingly, we discovered that XGBoost
319 outperformed the other models and emerged as the best classification model for both clinical targets.
320 The supervised ML models, designed to predict PPHN severity and neonatal mortality, showed
321 promising preliminary results. Our study suggests that predicting mortality and PPHN severity in the
322 prenatal and very early postnatal period can be feasible by ML applications, achieving accuracies of
323 88% for mortality and 82% for postnatal PPHN. With significant accuracy rates and reliable
324 sensitivity, this model has the potential to revolutionize prognostic assessment in CDH, eventually
325 improving patient outcomes. By implementing the algorithm, risk categories could be simulated
326 based on available prenatal data and assuming gestational age and estimated fetal weight at birth. The
327 algorithm could also be updated in real time at subsequent obstetric visits or based on the threat of

328 preterm delivery, as prematurity plays a significant role in survival, especially in infants with
329 underlying disease. This would assist with parenting counseling, birth planning, and postnatal care.
330 To the best of our knowledge, our studies are the first to explore the application of AI methods to
331 CDH [29,30].

332 Despite being encouraging, some limitations must be considered. First, the restricted dataset deriving
333 from the rarity of the condition represented the weakest point. An appropriate number of cases during
334 training/validation and data interpretation is crucial for ML applications. Potential strategies may
335 involve collaborating with other institutions and prospectively considering including future cases to
336 augment the study population. Another critical aspect is data inhomogeneity, specifically the lack of
337 a standard grayscale in the images. This would require a standardization procedure, after which gray-
338 level-based features could be used to increase ML quality for classification purposes. Nonetheless,
339 MRI standardization is a delicate process that involves profound changes in image gray levels, which
340 might even make ML procedures less accurate. Consequently, we preferred to simply discard ML
341 features based on the gray-level content of ROIs, only using shape features. Interestingly, no shape
342 features were selected for the mortality target, whereas clinical and shape variables were chosen for
343 the PPHN target. We can speculate that the information provided by the images is more closely related
344 to the structure and architecture of the lung parenchyma, which directly impacts the disease's
345 pathophysiology. On the other hand, mortality may be an indirect result of these structural alterations,
346 influenced by many factors. Although a conclusive interpretation is not yet possible, this aspect
347 deserves further investigation, and an increase in the study population and image optimization are
348 crucial. Finally, the retrospective data collection is largely affected by missing or inaccurate data and
349 may be time-consuming for the clinician. Standardized assessment and computerized data collection
350 could improve the dataset quality.

351

352 **CONCLUSIONS**

353

354 Although with limitations, with reasonable accuracy, a ML approach for predicting mortality and
355 PPHN severity of CDH newborns using prenatal and very early post-natal variables appears feasible.
356 Our results could pave the way for new AI applications in the neonatal field. They would enable risk-
357 adjusted analyses of outcomes, healthcare costs, and management strategies, ultimately improving
358 the overall quality of care.

359

360 **Statements and Declarations**

361 **Competing Interests:** The authors have no relevant financial or non-financial interests to disclose.

362

363 **Funding:** This study was (partially) funded by the Italian Ministry of Health - Current Research
364 IRCCS.

365

366 **Author Contributions:** L.C., I.A., G.D.N., G.R., I.B., D.C., and G.C. contributed to the study's
367 conception and design; L.C., I.A., G.D.N., G.R., I.B., D.C., G.C. (Giuseppe Como), N.P., and G.C.
368 (Giacomo Cavallaro) contributed to the study's methodology, investigation, and data curation; I.B.
369 contributed to manual segmentation; L.C., G.D.N., L.C., and D.C. contributed to ML and DL
370 analysis; L.C., G.D.N., and D.C. performed the statistical analysis; L.C., I.A., G.D.N., G.R., I.B.,
371 D.C., and G.C. (Giacomo Cavallaro) wrote the initial draft preparation of the manuscript; L.C., I.A.,
372 G.D.N., G.R., I.B., D.C., G.C. (Giuseppe Como), N.P., M.C., M.F., and G.C. (Giacomo Cavallaro)
373 wrote, reviewed, and edited the manuscript; L.C., G.D.N., and D.C. contributed to designing the
374 figures; G.D.N. and G.C. (Giacomo Cavallaro) contributed equally to the visualization of the
375 manuscript; G.D.N. and G.C. (Giacomo Cavallaro) contributed to the supervision and project
376 administration of the study. All authors have read and agreed to the published version of the
377 manuscript.

378

379 **Ethics approval**

380 The present study was conducted using the principles of good clinical practice and the Helsinki
381 Declaration. It was approved by the local ethics committee (Milan Area 2, Italy) with approval
382 number 800_2020bis. However, due to the study's retrospective nature, the Ethics Committee waived
383 informed consent. The study was registered at ClinicalTrials.gov with the identifier NCT04609163.

384

385 **Consent to participate**

386 Written informed consent was obtained from the parents.

387

388 **Conflicts of Interest**

389 The authors declare that the research was conducted without any commercial or financial
390 relationships that could be construed as a potential conflict of interest.

391

392 **References**

393

- 394 1. Russo FM, De Coppi P, Allegaert K, Toelen J, van der Veecken L, Attilakos G, et al. Current
395 and future antenatal management of isolated congenital diaphragmatic hernia. *Semin Fetal*
396 *Neonatal Med.* 2017;22: 383–390. doi:10.1016/j.siny.2017.11.002
- 397 2. Keijzer R, Liu J, Deimling J, Tibboel D, Post M. Dual-Hit Hypothesis Explains Pulmonary
398 Hypoplasia in the Nitrofen Model of Congenital Diaphragmatic Hernia. *Am J Pathol.*
399 2000;156: 1299–1306. doi:10.1016/S0002-9440(10)65000-6
- 400 3. Pierro M, Thébaud B. Understanding and treating pulmonary hypertension in congenital
401 diaphragmatic hernia. *Semin Fetal Neonatal Med.* 2014;19: 357–363.
402 doi:10.1016/j.siny.2014.09.008
- 403 4. Snoek KG, Greenough A, van Rosmalen J, Capolupo I, Schaible T, Ali K, et al. Congenital
404 Diaphragmatic Hernia: 10-Year Evaluation of Survival, Extracorporeal Membrane
405 Oxygenation, and Foetoscopic Endotracheal Occlusion in Four High-Volume Centres.

- 406 Neonatology. 2018;113: 63–68. doi:10.1159/000480451
- 407 5. Harting MT, Lally KP. The Congenital Diaphragmatic Hernia Study Group registry update.
408 Semin Fetal Neonatal Med. 2014;19: 370–375. doi:10.1016/j.siny.2014.09.004
- 409 6. Metkus AP, Filly RA, Stringer MD, Harrison MR, Adzick NS. Sonographic predictors of
410 survival in fetal diaphragmatic hernia. J Pediatr Surg. 1996;31: 148–152. doi:10.1016/S0022-
411 3468(96)90338-3
- 412 7. Jani J, Peralta CFA, Benachi A, Deprest J, Nicolaidis KH. Assessment of lung area in
413 fetuses with congenital diaphragmatic hernia. Ultrasound Obstet Gynecol. 2007;30: 72–76.
414 doi:10.1002/uog.4051
- 415 8. Mahieu-Caputo D, Sonigo P, Dommergues M, Fournet JC, Thalabard JC, Abarca C, et al.
416 Fetal lung volume measurement by magnetic resonance imaging in congenital diaphragmatic
417 hernia. BJOG An Int J Obstet Gynaecol. 2001;108: 863–868. doi:10.1111/j.1471-
418 0528.2001.00184.x
- 419 9. Bultez T, Quibel T, Bouhanna P, Popowski T, Resche-Rigon M, Rozenberg P. Angle of fetal
420 head progression measured using transperineal ultrasound as a predictive factor of vacuum
421 extraction failure. Ultrasound Obstet Gynecol. 2016;48: 86–91. doi:10.1002/uog.14951
- 422 10. Büsing KA, Kilian AK, Schaible T, Dinter DJ, Neff KW. MR Lung Volume in Fetal
423 Congenital Diaphragmatic Hernia: Logistic Regression Analysis—Mortality and
424 Extracorporeal Membrane Oxygenation. Radiology. 2008;248: 233–239.
425 doi:10.1148/radiol.2481070934
- 426 11. Ruano R, Lazar DA, Cass DL, Zamora IJ, Lee TC, Cassady CI, et al. Fetal lung volume and
427 quantification of liver herniation by magnetic resonance imaging in isolated congenital
428 diaphragmatic hernia. Ultrasound Obstet Gynecol. 2014;43: 662–669.
429 doi:10.1002/uog.13223
- 430 12. Cannie M, Jani J, Meersschaert J, Allegaert K, Done' E, Marchal G, et al. Prenatal prediction
431 of survival in isolated diaphragmatic hernia using observed to expected total fetal lung

- 432 volume determined by magnetic resonance imaging based on either gestational age or fetal
433 body volume. *Ultrasound Obstet Gynecol.* 2008;32: 633–639. doi:10.1002/uog.6139
- 434 13. Lazar DA, Ruano R, Cass DL, Moise KJ, Johnson A, Lee TC, et al. Defining “liver-up”:
435 does the volume of liver herniation predict outcome for fetuses with isolated left-sided
436 congenital diaphragmatic hernia? *J Pediatr Surg.* 2012;47: 1058–1062.
437 doi:10.1016/j.jpedsurg.2012.03.003
- 438 14. Cordier A -G., Jani JC, Cannie MM, Rodó C, Fabietti I, Persico N, et al. Stomach position in
439 prediction of survival in left-sided congenital diaphragmatic hernia with or without
440 fetoscopic endoluminal tracheal occlusion. *Ultrasound Obstet Gynecol.* 2015;46: 155–161.
441 doi:10.1002/uog.14759
- 442 15. Estimating disease severity of congenital diaphragmatic hernia in the first 5 minutes of life. *J*
443 *Pediatr Surg.* 2001;36: 141–145. doi:10.1053/jpsu.2001.20032
- 444 16. Brindle ME, Cook EF, Tibboel D, Lally PA, Lally KP. A Clinical Prediction Rule for the
445 Severity of Congenital Diaphragmatic Hernias in Newborns. *Pediatrics.* 2014;134: e413–
446 e419. doi:10.1542/peds.2013-3367
- 447 17. Schultz CM, DiGeronimo RJ, Yoder BA. Congenital diaphragmatic hernia: a simplified
448 postnatal predictor of outcome. *J Pediatr Surg.* 2007;42: 510–516.
449 doi:10.1016/j.jpedsurg.2006.10.043
- 450 18. Skarsgard ED, MacNab YC, Qiu Z, Little R, Lee SK. SNAP-II Predicts Mortality among
451 Infants with Congenital Diaphragmatic Hernia. *J Perinatol.* 2005;25: 315–319.
452 doi:10.1038/sj.jp.7211257
- 453 19. Jancelewicz T, Brindle ME. Prediction tools in congenital diaphragmatic hernia. *Semin*
454 *Perinatol.* 2020;44: 151165. doi:10.1053/j.semperi.2019.07.004
- 455 20. Masino AJ, Harris MC, Forsyth D, Ostapenko S, Srinivasan L, Bonafide CP, et al. Machine
456 learning models for early sepsis recognition in the neonatal intensive care unit using readily
457 available electronic health record data. Juarez JM, editor. *PLoS One.* 2019;14: e0212665.

- 458 doi:10.1371/journal.pone.0212665
- 459 21. Hamilton EF, Dyachenko A, Ciampi A, Maurel K, Warrick PA, Garite TJ. Estimating risk of
460 severe neonatal morbidity in preterm births under 32 weeks of gestation. *J Matern Neonatal*
461 *Med.* 2020;33: 73–80. doi:10.1080/14767058.2018.1487395
- 462 22. Mani S, Ozdas A, Aliferis C, Varol HA, Chen Q, Carnevale R, et al. Medical decision
463 support using machine learning for early detection of late-onset neonatal sepsis. *J Am Med*
464 *Inform Assoc.* 2014;21: 326–36. doi:10.1136/amiajnl-2013-001854
- 465 23. Kumaresan D, Stephenson J, Doxey AC, Bandukwala H, Brooks E, Hillebrand-Voiculescu
466 A, et al. Aerobic proteobacterial methylotrophs in Movile Cave: genomic and metagenomic
467 analyses. *Microbiome.* 2018;6: 1. doi:10.1186/s40168-017-0383-2
- 468 24. Azevedo RSS, de Sousa JR, Araujo MTF, Martins Filho AJ, de Alcantara BN, Araujo FMC,
469 et al. In situ immune response and mechanisms of cell damage in central nervous system of
470 fatal cases microcephaly by Zika virus. *Sci Rep.* 2018;8: 1. doi:10.1038/s41598-017-17765-5
- 471 25. Cooper JN, Minneci PC, Deans KJ. Postoperative neonatal mortality prediction using
472 superlearning. *J Surg Res.* 2018;221: 311–319. doi:10.1016/j.jss.2017.09.002
- 473 26. Irles C, González-Pérez G, Carrera Muiños S, Michel Macias C, Sánchez Gómez C,
474 Martínez-Zepeda A, et al. Estimation of Neonatal Intestinal Perforation Associated with
475 Necrotizing Enterocolitis by Machine Learning Reveals New Key Factors. *Int J Environ Res*
476 *Public Health.* 2018;15. doi:10.3390/ijerph15112509
- 477 27. Masino AJ, Harris MC, Forsyth D, Ostapenko S, Srinivasan L, Bonafide CP, et al. Machine
478 learning models for early sepsis recognition in the neonatal intensive care unit using readily
479 available electronic health record data. *PLoS One.* 2019;14: e0212665.
480 doi:10.1371/journal.pone.0212665
- 481 28. Hamilton EF, Dyachenko A, Ciampi A, Maurel K, Warrick PA, Garite TJ. Estimating risk of
482 severe neonatal morbidity in preterm births under 32 weeks of gestation. *J Matern Fetal*
483 *Neonatal Med.* 2020;33: 73–80. doi:10.1080/14767058.2018.1487395

- 484 29. Amodeo I, De Nunzio G, Raffaelli G, Borzani I, Griggio A, Conte L, et al. A maChine and
485 deep Learning Approach to predict pulmoNary hyperteNsIon in newbornS with congenital
486 diaphragmatic Hernia (CLANNISH): Protocol for a retrospective study. PLoS One. 2021;16:
487 e0259724. doi:10.1371/journal.pone.0259724
- 488 30. Conte L, Amodeo I, De Nunzio G, Raffaelli G, Borzani I, Persico N, et al. Congenital
489 diaphragmatic hernia: automatic lung and liver MRI segmentation with nnU-Net,
490 reproducibility of pyradiomics features, and a machine learning application for the
491 classification of liver herniation. Eur J Pediatr. 2024. doi:10.1007/s00431-024-05476-9
- 492 31. Rypens F, Metens T, Rocourt N, Sonigo P, Brunelle F, Quere MP, et al. Fetal Lung Volume:
493 Estimation at MR Imaging—Initial Results. Radiology. 2001;219: 236–241.
494 doi:10.1148/radiology.219.1.r01ap18236
- 495 32. Zizka J, Elias P, Hodik K, Tintera J, Juttnerova V, Belobradek Z, et al. Liver, meconium,
496 haemorrhage: the value of T1-weighted images in fetal MRI. Pediatr Radiol. 2006;36: 792–
497 801. doi:10.1007/s00247-006-0239-6
- 498 33. van Griethuysen JJM, Fedorov A, Parmar C, Hosny A, Aucoin N, Narayan V, et al.
499 Computational Radiomics System to Decode the Radiographic Phenotype. Cancer Res.
500 2017;77: e104–e107. doi:10.1158/0008-5472.CAN-17-0339
- 501 34. Xiao Z, Gong K, Zou Y. A combined forecasting approach based on fuzzy soft sets. J
502 Comput Appl Math. 2009;228: 326–333. doi:10.1016/j.cam.2008.09.033
- 503 35. Thanh Noi P, Kappas M. Comparison of Random Forest, k-Nearest Neighbor, and Support
504 Vector Machine Classifiers for Land Cover Classification Using Sentinel-2 Imagery.
505 Sensors. 2017;18: 18. doi:10.3390/s18010018
- 506 36. Doyle NM, Lally KP. The CDH study group and advances in the clinical care of the patient
507 with congenital diaphragmatic hernia. Semin Perinatol. 2004;28: 174–184.
508 doi:10.1053/j.semperi.2004.03.009
- 509 37. Long A-M, Bunch KJ, Knight M, Kurinczuk JJ, Losty PD. One-year outcomes of infants

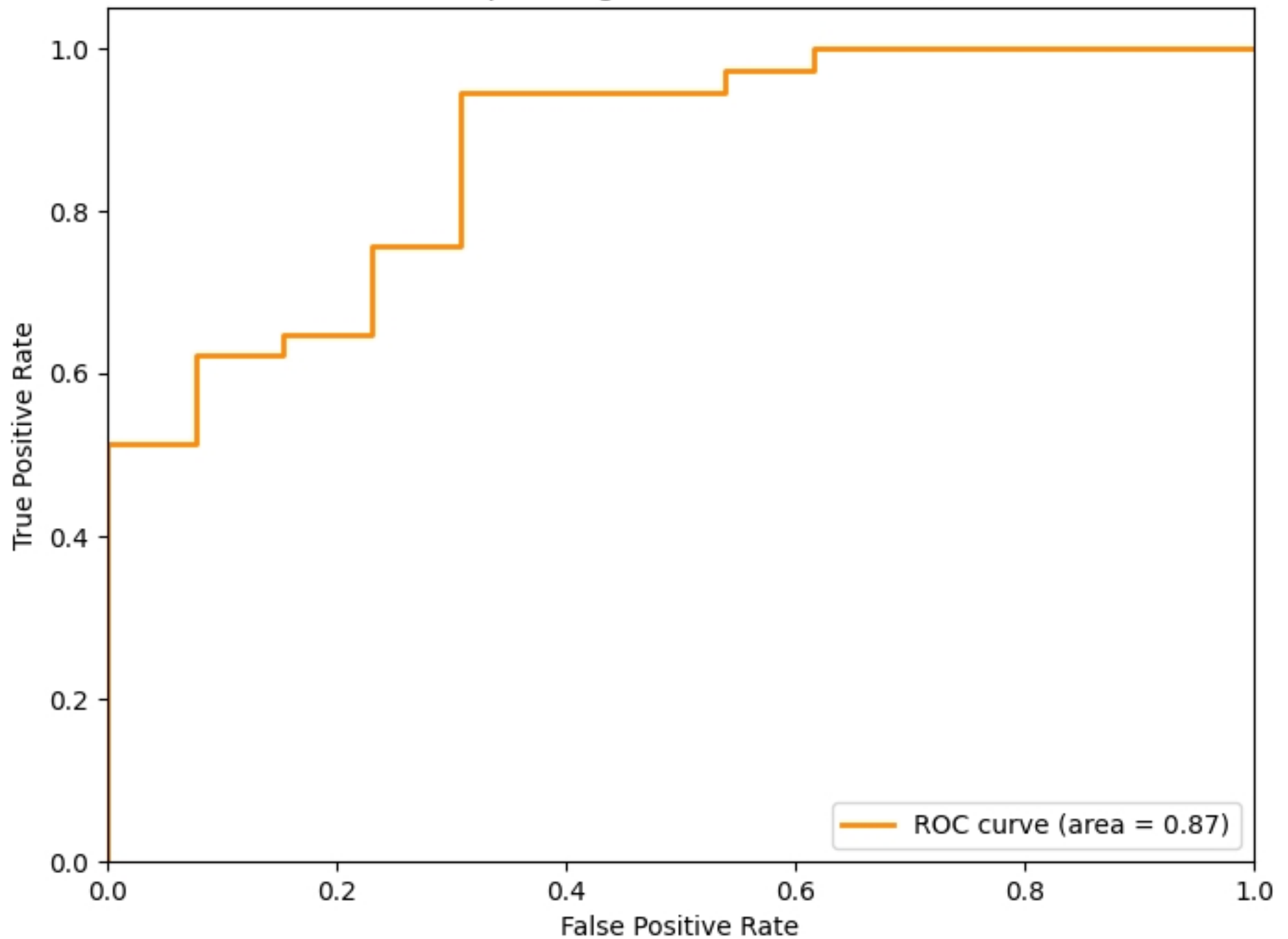
- 510 born with congenital diaphragmatic hernia: a national population cohort study. *Arch Dis*
511 *Child - Fetal Neonatal Ed.* 2019;104: F643–F647. doi:10.1136/archdischild-2018-316396
- 512 38. Cochius-den Otter SCM, Erdem Ö, van Rosmalen J, Schaible T, Peters NCJ, Cohen-
513 Overbeek TE, et al. Validation of a Prediction Rule for Mortality in Congenital
514 Diaphragmatic Hernia. *Pediatrics.* 2020;145. doi:10.1542/peds.2019-2379
- 515 39. Kipfmüller F, Schroeder L, Melaku T, Geipel A, Berg C, Gembruch U, et al. Prediction of
516 ECMO and Mortality in Neonates with Congenital Diaphragmatic Hernia Using the SNAP-II
517 Score. *Klin Pädiatrie.* 2019;231: 297–303. doi:10.1055/a-1009-6671
- 518 40. Montalva L, Raffler G, Riccio A, Lauriti G, Zani A. Neurodevelopmental impairment in
519 children with congenital diaphragmatic hernia: Not an uncommon complication for
520 survivors. *J Pediatr Surg.* 2020;55: 625–634. doi:10.1016/j.jpedsurg.2019.05.021
- 521 41. Kinsella JP, Steinhorn RH, Mullen MP, Hopper RK, Keller RL, Ivy DD, et al. The Left
522 Ventricle in Congenital Diaphragmatic Hernia: Implications for the Management of
523 Pulmonary Hypertension. *J Pediatr.* 2018;197: 17–22. doi:10.1016/j.jpeds.2018.02.040
- 524 42. Massolo AC, Paria A, Hunter L, Finlay E, Davis CF, Patel N. Ventricular Dysfunction,
525 Interdependence, and Mechanical Dispersion in Newborn Infants with Congenital
526 Diaphragmatic Hernia. *Neonatology.* 2019;116: 68–75. doi:10.1159/000499347
- 527 43. Gien J, Kinsella JP. Management of pulmonary hypertension in infants with congenital
528 diaphragmatic hernia. *J Perinatol.* 2016;36: S28–S31. doi:10.1038/jp.2016.46
- 529 44. Mank A, Carrasco Carrasco C, Thio M, Clotet J, Pauws SC, DeKoninck P, et al. Tidal
530 volumes at birth as predictor for adverse outcome in congenital diaphragmatic hernia. *Arch*
531 *Dis Child - Fetal Neonatal Ed.* 2020;105: 248–252. doi:10.1136/archdischild-2018-316504
- 532 45. Oh C, Youn JK, Han J, Yang H, Lee S, Seo J, et al. Predicting Survival of Congenital
533 Diaphragmatic Hernia on the First Day of Life. *World J Surg.* 2019;43: 282–290.
534 doi:10.1007/s00268-018-4780-x
- 535 46. Brown BP, Clark MT, Wise RL, Timsina LR, Reher TA, Vandewalle RJ, et al. A

- 536 multifactorial severity score for left congenital diaphragmatic hernia in a high-risk population
537 using fetal magnetic resonance imaging. *Pediatr Radiol.* 2019;49: 1718–1725.
538 doi:10.1007/s00247-019-04478-2
- 539 47. Dassios T, Ali K, Makin E, Bhat R, Krokidis M, Greenough A. Prediction of Mortality in
540 Newborn Infants With Severe Congenital Diaphragmatic Hernia Using the Chest
541 Radiographic Thoracic Area*. *Pediatr Crit Care Med.* 2019;20: 534–539.
542 doi:10.1097/PCC.0000000000001912
- 543 48. Jani J, Nicolaidis KH, Keller RL, Benachi A, Peralta CFA, Favre R, et al. Observed to
544 expected lung area to head circumference ratio in the prediction of survival in fetuses with
545 isolated diaphragmatic hernia. *Ultrasound Obstet Gynecol.* 2007;30: 67–71.
546 doi:10.1002/uog.4052
- 547 49. Snoek KG, Peters NCJ, van Rosmalen J, van Heijst AFJ, Eggink AJ, Sikkel E, et al. The
548 validity of the observed-to-expected lung-to-head ratio in congenital diaphragmatic hernia in
549 an era of standardized neonatal treatment; a multicenter study. *Prenat Diagn.* 2017;37: 658–
550 665. doi:10.1002/pd.5062
- 551 50. Amodeo I, Borzani I, Raffaeli G, Persico N, Amelio GS, Gulden S, et al. The role of
552 magnetic resonance imaging in the diagnosis and prognostic evaluation of fetuses with
553 congenital diaphragmatic hernia. *Eur J Pediatr.* 2022;181: 3243–3257. doi:10.1007/s00431-
554 022-04540-6
- 555 51. Victoria T, Bebbington MW, Danzer E, Flake AW, Johnson MP, Dinan D, et al. Use of
556 magnetic resonance imaging in prenatal prognosis of the fetus with isolated left congenital
557 diaphragmatic hernia. *Prenat Diagn.* 2012;32: 715–23. doi:10.1002/pd.3890
- 558 52. Dütemeyer V, Cordier A-G, Cannie MM, Bevilacqua E, Huynh V, Houfflin-Debarge V, et al.
559 Prenatal prediction of postnatal survival in fetuses with congenital diaphragmatic hernia
560 using MRI: lung volume measurement, signal intensity ratio, and effect of experience. *J*
561 *Matern Fetal Neonatal Med.* 2022;35: 1036–1044. doi:10.1080/14767058.2020.1740982

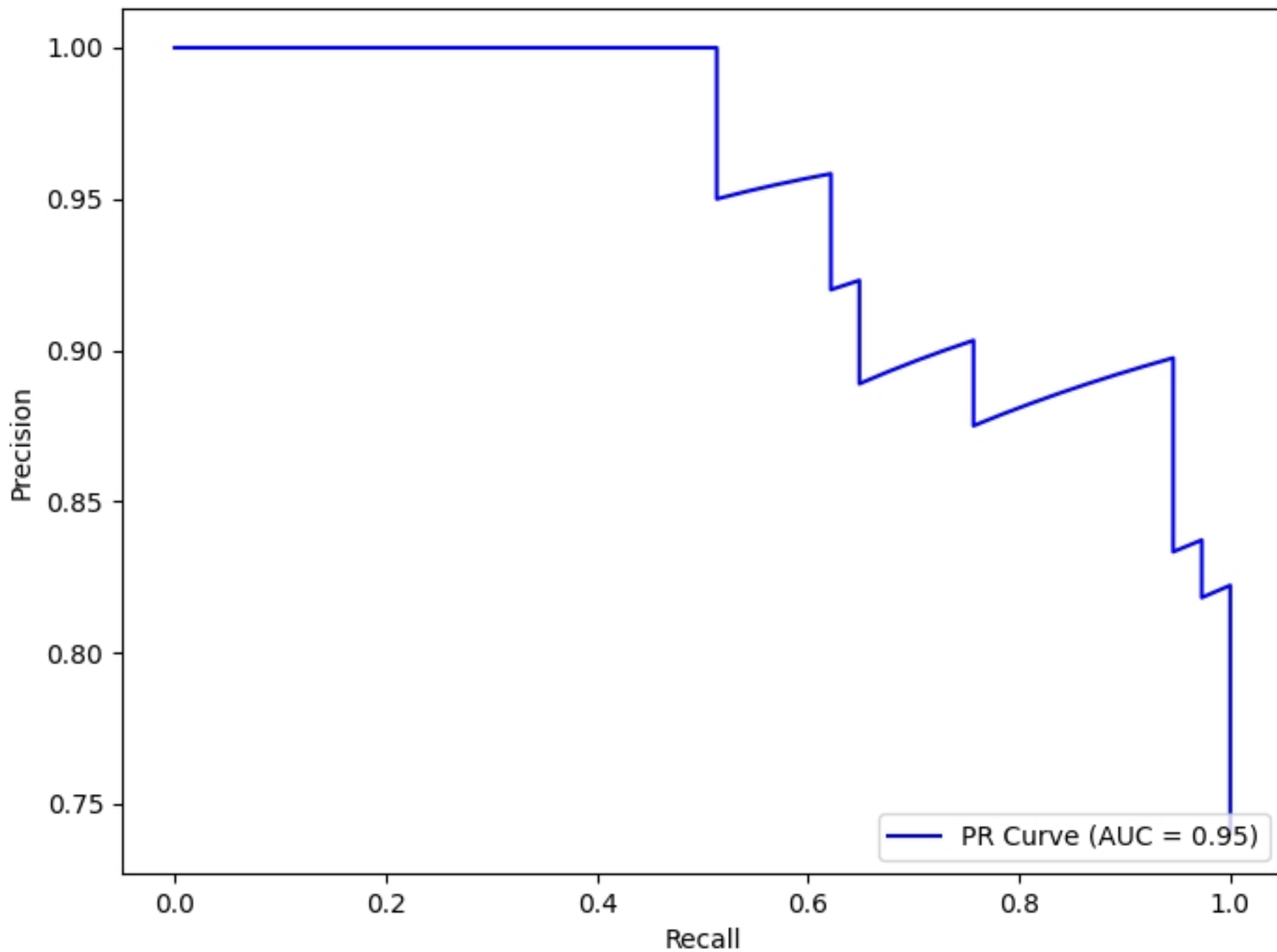
- 562 53. Jani J, Cannie M, Done E, Van Mieghem T, Van Schoubroeck D, Gucciardo L, et al.
563 Relationship between lung area at ultrasound examination and lung volume assessment with
564 magnetic resonance imaging in isolated congenital diaphragmatic hernia. *Ultrasound Obstet*
565 *Gynecol.* 2007;30: 855–60. doi:10.1002/uog.5168
- 566 54. Jani J, Cannie M, Sonigo P, Robert Y, Moreno O, Benachi A, et al. Value of prenatal
567 magnetic resonance imaging in the prediction of postnatal outcome in fetuses with
568 diaphragmatic hernia. *Ultrasound Obstet Gynecol.* 2008;32: 793–9. doi:10.1002/uog.6234
- 569 55. Bebbington M, Victoria T, Danzer E, Moldenhauer J, Khalek N, Johnson M, et al.
570 Comparison of ultrasound and magnetic resonance imaging parameters in predicting survival
571 in isolated left-sided congenital diaphragmatic hernia. *Ultrasound Obstet Gynecol.* 2014;43:
572 670–4. doi:10.1002/uog.13271
- 573 56. Oluyomi-Obi T, Kuret V, Puligandla P, Lodha A, Lee-Robertson H, Lee K, et al. Antenatal
574 predictors of outcome in prenatally diagnosed congenital diaphragmatic hernia (CDH). *J*
575 *Pediatr Surg.* 2017;52: 881–888. doi:10.1016/j.jpedsurg.2016.12.008
- 576 57. Petroze RT, Caminsky NG, Trebichavsky J, Bouchard S, Le-Nguyen A, Laberge J-M, et al.
577 Prenatal prediction of survival in congenital diaphragmatic hernia: An audit of postnatal
578 outcomes. *J Pediatr Surg.* 2019;54: 925–931. doi:10.1016/j.jpedsurg.2019.01.021
- 579 58. Neff KW, Kilian AK, Schaible T, Schütz E-M, Büsing KA. Prediction of mortality and need
580 for neonatal extracorporeal membrane oxygenation in fetuses with congenital diaphragmatic
581 hernia: logistic regression analysis based on MRI fetal lung volume measurements. *AJR Am*
582 *J Roentgenol.* 2007;189: 1307–11. doi:10.2214/AJR.07.2434
- 583 59. Lee TC, Lim FY, Keswani SG, Frischer JS, Haberman B, Kingma PS, et al. Late gestation
584 fetal magnetic resonance imaging-derived total lung volume predicts postnatal survival and
585 need for extracorporeal membrane oxygenation support in isolated congenital diaphragmatic
586 hernia. *J Pediatr Surg.* 2011;46: 1165–71. doi:10.1016/j.jpedsurg.2011.03.046
- 587 60. Alfaraj MA, Shah PS, Bohn D, Pantazi S, O'Brien K, Chiu PP, et al. Congenital

- 588 diaphragmatic hernia: lung-to-head ratio and lung volume for prediction of outcome. *Am J*
589 *Obstet Gynecol.* 2011;205: 43.e1–8. doi:10.1016/j.ajog.2011.02.050
- 590 61. Russo FM, Eastwood MP, Keijzer R, Al-Maary J, Toelen J, Van Mieghem T, et al. Lung size
591 and liver herniation predict need for extracorporeal membrane oxygenation but not
592 pulmonary hypertension in isolated congenital diaphragmatic hernia: systematic review and
593 meta-analysis. *Ultrasound Obstet Gynecol.* 2017;49: 704–713. doi:10.1002/uog.16000
- 594 62. Walleyo A, Debus A, Kehl S, Weiss C, Schönberg SO, Schaible T, et al. Periodic MRI lung
595 volume assessment in fetuses with congenital diaphragmatic hernia: prediction of survival,
596 need for ECMO, and development of chronic lung disease. *AJR Am J Roentgenol.* 2013;201:
597 419–26. doi:10.2214/AJR.12.8655
- 598 63. Büsing KA, Kilian AK, Schaible T, Endler C, Schaffelder R, Neff KW. MR relative fetal
599 lung volume in congenital diaphragmatic hernia: survival and need for extracorporeal
600 membrane oxygenation. *Radiology.* 2008;248: 240–6. doi:10.1148/radiol.2481070952
- 601 64. Schaible T, Büsing KA, Felix JF, Hop WCJ, Zahn K, Wessel L, et al. Prediction of chronic
602 lung disease, survival and need for ECMO therapy in infants with congenital diaphragmatic
603 hernia: additional value of fetal MRI measurements? *Eur J Radiol.* 2012;81: 1076–82.
604 doi:10.1016/j.ejrad.2011.02.060
605

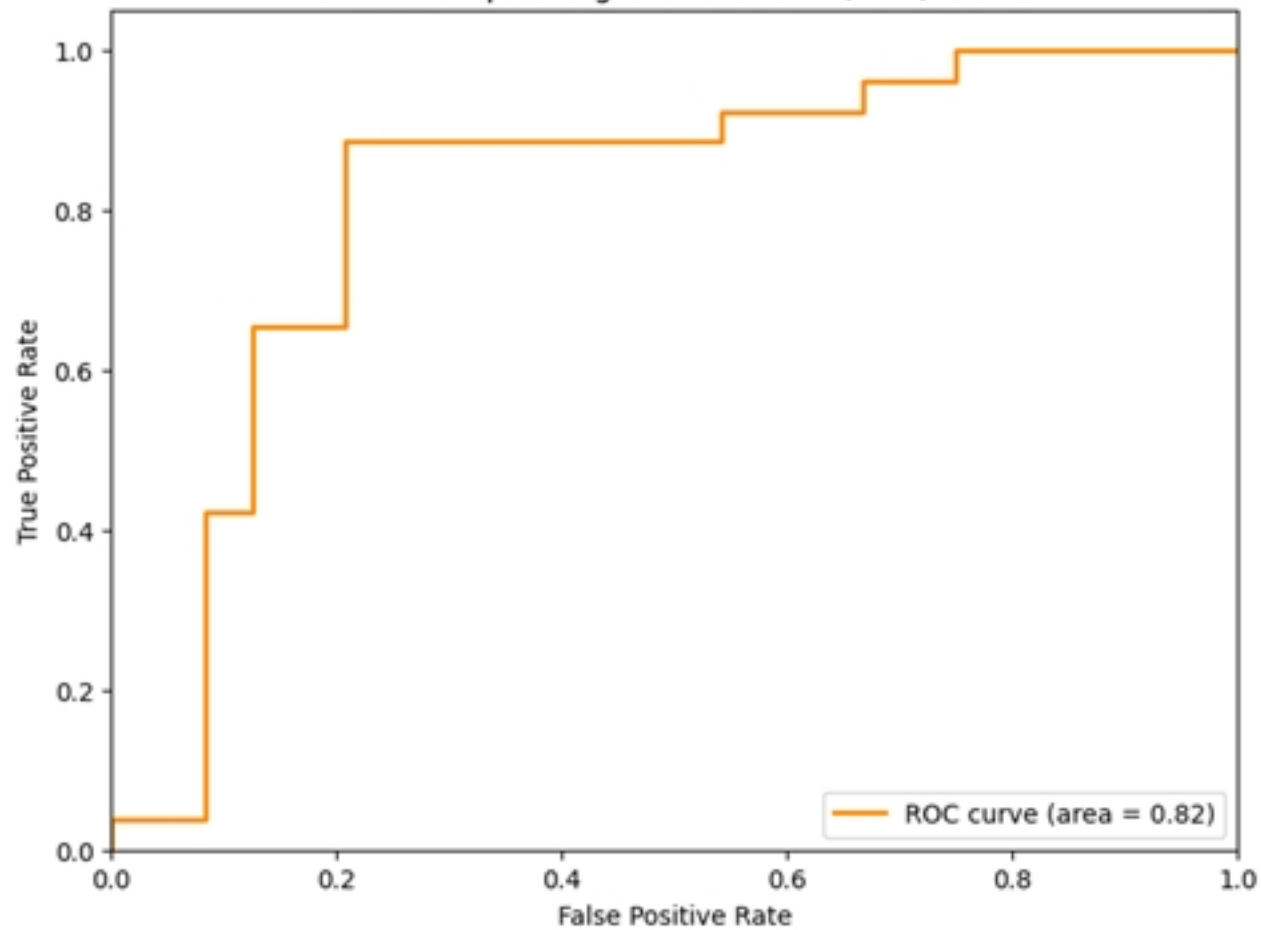
Receiver Operating Characteristic (ROC) Curve



Precision-Recall Curve



Receiver Operating Characteristic (ROC) Curve



Precision-Recall Curve

